Adaptive Backstepping Control of a 2-DOF Helicopter System with Uniform Quantized Inputs

Siri Marte Schlanbusch
Department of Engineering Sciences
University of Agder
Grimstad, Norway 4879
siri.schlanbusch@uia.no

Jing Zhou
Department of Engineering Sciences
University of Agder
Grimstad, Norway 4879
jing.zhou@uia.no

***Abstract*—This paper proposes a new adaptive controller for a 2-Degree of Freedom (DOF) helicopter system in the presence of input quantization. The inputs are quantized by uniform quantizers. A nonlinear mathematical model is derived for the 2-DOF helicopter system based on Euler-Lagrange equations, where the system parameters and the control coefficients are uncertain. A new adaptive control algorithm is developed by using backstepping technique to track the pitch and yaw position references independently. Only quantized input signals are used in the system which reduces communication rate and cost. It is shown that not only the ultimate stability is guaranteed by the proposed controller, but also the designers can tune the design parameters in an explicit way to obtain the required closed loop behavior. Experiments are carried out on the Quanser helicopter system to validate the effectiveness, robustness and control capability of the proposed scheme.**

***Index Terms*—Adaptive control, backstepping, 2-degree of freedom helicopter, quantization, position control**

I. Introduction

The development and interest of distributed and networked control systems (NCSs) have increased recent years, where a control system involves a communication network [1]–[3]. There are several advantages of networked systems such as reduced wiring and easier maintenance, and with numerous applications e.g. as smart grids and unmanned aerial vehicles. Communication networks also give rise to some disadvantages such as networked-induced delays, packet dropouts and quantization. In a communication network the channel capacity may be limited, restricting number of bits that can be transmitted over the network, and digital rather than continuous signals are used when transmitting data. Quantization is often used for the discontinuous mapping from a continuous space to a finite set. It is nonlinear, since several different input signals can give the same output and is an irreversible process. This introduces nonlinear errors in the control loop.

Due to its importance, quantized control has received a lot of attention, and it is of interest to see how it will affect the stability of a system. In [4]–[6] control of linear and nonlinear systems were looked at where either the input, output or the state were quantized. Quantized feedback control was considered in [7] for linear single-input-single-output (SISO) and multiple-input-multiple-output (MIMO) systems, where optimal control and robust control were used for performance purposes. Quantized control for stability of a nonlinear system with uncertainties was considered in [8] using a robust approach, and adaptive approaches have been studied in [9]–[13]. Here the backstepping technique was used in the control design, and different quantizers were considered including uniform, logarithmic and hysteresis and where either the inputs or the states were quantized. Adaptive control was also considered in [14] for nonlinear MIMO systems with input quantization.

The backstepping technique was proposed in the 1990's, and is a nonlinear controller design method where the control input is designed to compensate for the effects of plant nonlinearity [15]. It has been widely used to design adaptive controllers for uncertain systems, where the controller has a dynamic feedback for estimating the parameters in form of an adaptive update law. This technique has several advantages over the conventional approaches such as providing a promising way to improve the transient performance of adaptive systems by tuning design parameters.

In this paper, a 2-degree-of-freedom (DOF) helicopter system is considered, where the inputs are quantized. It is a nonlinear MIMO system, with challenges in controller design due to its nonlinear behavior, its coupling, and with uncertainties both in the model and the parameters, and with disturbance from the quantized inputs. We consider the adaptive backstepping controller for this system as in [16], where a theoretical proof of stability was given with the use of constructed Lyapunov functions, and where tracking was achieved and also boundedness of all signals in the closed loop system. It was also shown that the tracking error performance can be improved by adjusting the design parameters. This paper extends the results to include quantization of the inputs using a uniform quantization and prove boundedness of the closed loop signals.

The following notations are used. Vectors are denoted by small bold letters and matrices with capitalized bold letters. When the context is sufficient explicit, we may omit to write arguments of a function, vector or matrix.

The paper is organized as follows. In Section II the system model, the quantized feedback system and the uniform quantizer are presented. Section III presents the adaptive control design based on backstepping technique with stability and performance results, Section IV presents the experimental results before the conclusion is given in Section V.

II. Problem statement

A. System model

The helicopter system is visualized in Figure 1 showing both a free body diagram (FBD) and a kinetic diagram (KD). The main motor is producing two forces, one main force, F_{Mz}, in the z_b-direction that will give a positive pitch angle, and also a force, F_{My}, in the y_b-direction, meaning this will give a yaw angle. This last force is due to the aerodynamic forces. The tail motor is also producing two forces, F_{Tz} and F_{Ty}. This motor is basically here to counteract the yaw from the main motor and thus control the yaw while the main motor is controlling the pitch. These forces are functions of the two system inputs, u_1 and u_2, that are the voltages applied to the main and tail motors. Viscous damping, proportional to the velocity of the Aero body, is also present.

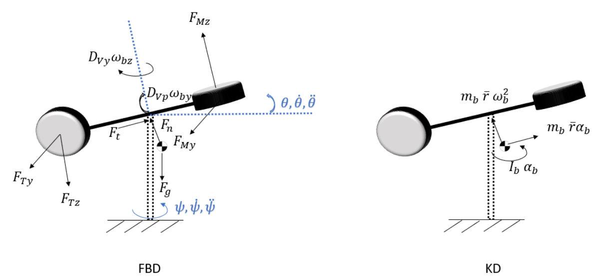

Fig. 1. Free body diagram and kinetic diagram of the Aero body

This is a MIMO system with 2 DOF, where each input will change both the pitch and yaw angle. The helicopter model is considered as a rigid body and the equations of motion are derived using Euler-Lagrange equations as given in [16], where the system parameters and control coefficients are uncertain.

The state variables are defined as

$$\boldsymbol{x} = [\vartheta(t), \psi(t), \dot{\vartheta}(t), \dot{\psi}(t)]^\top, \tag{1}$$

where ϑ and ψ are pitch and yaw angles, and $\dot{\vartheta}$ and $\dot{\psi}$ are angular velocities of pitch and yaw angles. The control variables are defined as

$$\boldsymbol{u} = [u_1(t, \boldsymbol{x}), u_2(t, \boldsymbol{x})]^\top, \tag{2}$$

and are the inputs that will be quantized. The nonlinear state space model is expressed as

$$\dot{\boldsymbol{x}} = \begin{bmatrix} x_3 \\ x_4 \\ \boldsymbol{\phi}_1^\top \boldsymbol{\theta}_1 \\ \boldsymbol{\phi}_2^\top \boldsymbol{\theta}_2 \end{bmatrix} + \begin{bmatrix} 0 \\ 0 \\ \beta_{1,1} u_1 + \beta_{1,2} u_2 \\ -\beta_{2,1} u_1 + \beta_{2,2} u_2 \end{bmatrix} \tag{3}$$

where $\boldsymbol{\phi}_1$ and $\boldsymbol{\phi}_2$ are known nonlinear functions defined as

$$\boldsymbol{\phi}_1 = \begin{bmatrix} -x_3 \\ -\sin x_1 \\ x_4^2 \cos x_1 \sin x_1 \end{bmatrix}, \quad \boldsymbol{\phi}_2 = \begin{bmatrix} -x_4 \\ -x_2 x_4 \cos x_1 \sin x_1 \end{bmatrix}, \tag{4}$$

vectors $\boldsymbol{\theta}_1$ and $\boldsymbol{\theta}_2$ are unknown constant vectors defined as

$$\boldsymbol{\theta}_1 = \frac{1}{I_p + ml_{cm}^2} \begin{bmatrix} D_{Vp} \\ mgl_{cm} \\ ml_{cm}^2 \end{bmatrix}, \quad \boldsymbol{\theta}_2 = \frac{1}{I_y} \begin{bmatrix} D_{Vy} \\ 2ml_{cm}^2 \end{bmatrix}, \tag{5}$$

and $\boldsymbol{\beta}_{i,j},\ i, j \in \{1, 2\}$, are unknown constants defined as

$$\beta_{1,1} = \frac{K_{pp}}{I_p + ml_{cm}^2}, \qquad \beta_{1,2} = \frac{K_{py}}{I_p + ml_{cm}^2}, \tag{6}$$

$$\beta_{2,1} = \frac{K_{yp}}{I_y}, \qquad \beta_{2,2} = \frac{K_{yy}}{I_y}. \tag{7}$$

The constants K_{pp} and K_{yy} are torque thrust gains from main and tail motors, K_{py} is cross-torque thrust gain acting on pitch from tail motor, K_{yp} is cross-torque thrust gain acting on yaw from main motor, l_{cm} is the distance between the center of mass and the origin of the body-fixed frame, I_p and I_y are the moments of inertia of the pitch and yaw respectively, g is the gravity acceleration, m is the total mass of the Aero body, and D_{V_y} and D_{V_p} are the damping constants for the rotation along the yaw axis and pitch axis separately.

The control objective is to design a control law for u_1 and u_2 to force the outputs x_1 and x_2 to track the reference signals $x_{r1}(t)$ and $x_{r2}(t)$ for pitch and yaw respectively when the inputs are quantized. To achieve the objective, the following assumptions are imposed.

Assumption 1: The reference signals x_{r1} and x_{r2} and first and second order derivatives are known, piecewise continuous and bounded.

Assumption 2: All unknown parameters $\boldsymbol{\theta}_1, \boldsymbol{\theta}_2, \beta_{i,j},\ i, j \in \{1, 2\}$ are positive constants and within known bounds.

B. Quantized System

In this paper, we consider a quantized feedback system as shown in Figure 2. The inputs u_1 and u_2 in system (3) take the quantized values, that are quantized at the encoder side.

C. Uniform Quantizer

The control inputs u_1 and u_2 are quantized using a uniform quantizer which has intervals of fixed lengths and is defined as follows:

$$q(u_k) = \begin{cases} u_{k,i} \operatorname{sgn}(u_k), & u_{k,i} - \frac{l_k}{2} \leq |u_k| < u_{k,i} + \frac{l_k}{2} \\ 0, & |u_k| < u_{k,0} + \frac{l_k}{2} \end{cases} \tag{8}$$

where $k = 1, 2$, $u_{k,0} > -l_k/2$ is a constant, $l_k > 0$ is the length of the quantization intervals, $i = 1, 2, ...$, and $u_{k,i+1} = u_{k,i} + l_k$. The uniform quantization $q(u_k) \in U_k = \{0, \pm u_{k,i}\}$, and a map of the quantization for $u_k > 0$ is shown in Figure 3.

The smaller the quantization intervals are, the closer the signal is to its continuous counterpart.

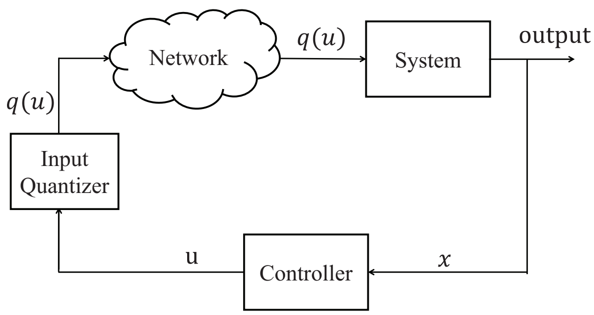

Fig. 2. System with quantized inputs

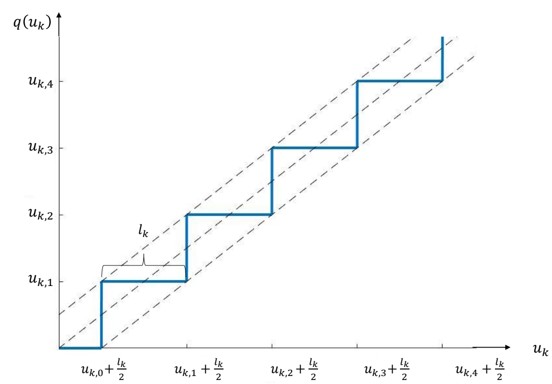

Fig. 3. Map of the uniform quantization, for $u_k > 0$

III. Adaptive Control Design

In this section, we will design adaptive feedback control laws for the helicopter model using backstepping technique. First considering the case when the inputs are continuous and then with quantized inputs.

A. Continuous Inputs

We begin by introducing the change of coordinates

$$z_1 = x_1 - x_{r1}, \tag{9}$$
$$z_2 = x_2 - x_{r2}, \tag{10}$$
$$z_3 = x_3 - \alpha_1 - \dot{x}_{r1}, \tag{11}$$
$$z_4 = x_4 - \alpha_2 - \dot{x}_{r2}. \tag{12}$$

where α_1 and α_2 are the virtual controllers. The design follows the backstepping procedure in [15].

• *Step* 1: The virtual controllers are chosen as

$$\alpha_1 = -c_1 z_1, \tag{13}$$
$$\alpha_2 = -c_2 z_2, \tag{14}$$

where c_1 and c_2 are positive constants. A control Lyapunov function is chosen as

$$V_1(\boldsymbol{z}, t) = \frac{1}{2} z_1^2 + \frac{1}{2} z_2^2. \tag{15}$$

The derivative of V_1 along the solutions of the system is

$$\begin{aligned} \dot{V}_1 &= z_1 \dot{z}_1 + z_2 \dot{z}_2 \\ &= z_1(z_3 + \alpha_1) + z_2(z_4 + \alpha_2) \\ &= -c_1 z_1^2 + z_1 z_3 - c_2 z_2^2 + z_2 z_4. \end{aligned} \tag{16}$$

If z_3 and z_4 are zero, then $\dot{V}_1$ is negative and z_1 and z_2 will converge exponentially towards zero.

• *Step* 2: The derivative of z_3 and z_4 are expressed as

$$\dot{z}_3 = \beta_{1,1} u_1 + \beta_{1,2} u_2 + \boldsymbol{\phi}_1^\top \boldsymbol{\theta}_1 + c_1(x_3 - \dot{x}_{r1}) - \ddot{x}_{r1}, \tag{17}$$
$$\dot{z}_4 = -\beta_{2,1} u_1 + \beta_{2,2} u_2 + \boldsymbol{\phi}_2^\top \boldsymbol{\theta}_2 + c_2(x_4 - \dot{x}_{r2}) - \ddot{x}_{r2}. \tag{18}$$

The control inputs u_1 and u_2 will now be designed so that z_1, z_2, z_3 and z_4 all converge towards zero.

The adaptive control law is designed as follows:

$$\boldsymbol{u} = \begin{bmatrix} u_1 \\ u_2 \end{bmatrix} = \hat{\boldsymbol{B}}^{-1} \bar{\boldsymbol{u}} = \hat{\boldsymbol{R}} \bar{\boldsymbol{u}}, \tag{19}$$

where

$$\bar{\boldsymbol{u}} = \begin{bmatrix} \bar{u}_1 \\ \bar{u}_2 \end{bmatrix}, \quad \hat{\boldsymbol{B}} = \begin{bmatrix} \hat{\boldsymbol{\beta}}_1 \\ \hat{\boldsymbol{\beta}}_2 \end{bmatrix}, \tag{20}$$
$$\bar{u}_1 = - z_1 - \boldsymbol{\phi}_1^\top \hat{\boldsymbol{\theta}}_1 - c_3 z_3 - c_1(x_3 - \dot{x}_{r1}) + \ddot{x}_{r1}, \tag{21}$$
$$\bar{u}_2 = - z_2 - \boldsymbol{\phi}_2^\top \hat{\boldsymbol{\theta}}_2 - c_4 z_4 - c_2 (x_4 - \dot{x}_{r2}) + \ddot{x}_{r2}, \tag{22}$$
$$\hat{\boldsymbol{\beta}}_1 = \begin{bmatrix} \hat{\beta}_{1,1} & \hat{\beta}_{1,2} \end{bmatrix}, \quad \hat{\boldsymbol{\beta}}_2 = \begin{bmatrix} -\hat{\beta}_{2,1} & \hat{\beta}_{2,2} \end{bmatrix}, \tag{23}$$

c_3 and c_4 are positive constants, $\hat{\boldsymbol{\theta}}_1$, $\hat{\boldsymbol{\theta}}_2$, $\hat{\beta}_{i,j}$ are the estimates of $\boldsymbol{\theta}_1$, $\boldsymbol{\theta}_2$, $\beta_{i,j}$ and $\hat{\boldsymbol{R}}$ is the inverse of the matrix $\hat{\boldsymbol{B}}$.

The parameter updating laws are chosen as

$$\dot{\hat{\boldsymbol{\theta}}}_1 = \mathrm{Proj}\{\boldsymbol{\Gamma}_1 \boldsymbol{\phi}_1 z_3\}, \tag{24}$$
$$\dot{\hat{\boldsymbol{\theta}}}_2 = \mathrm{Proj}\{\boldsymbol{\Gamma}_2 \boldsymbol{\phi}_2 z_4\}, \tag{25}$$
$$\dot{\hat{\boldsymbol{\beta}}}_1^\top = \mathrm{Proj}\{\boldsymbol{\Gamma}_3 \boldsymbol{u} z_3\}, \tag{26}$$
$$\dot{\hat{\boldsymbol{\beta}}}_2^\top = \mathrm{Proj}\{\boldsymbol{\Gamma}_4 \boldsymbol{u} z_4\}, \tag{27}$$

where $\boldsymbol{\Gamma}_k$, $k \in \{1, 2, 3, 4\}$, are positive definite adaptation gain matrices and $\mathrm{Proj}\{\cdot\}$ is the projection operator given in [15] which ensures that the estimates and estimation errors are nonzero and within known bounds. Let $\tilde{\boldsymbol{\theta}}_i = \boldsymbol{\theta}_i - \hat{\boldsymbol{\theta}}_i$ and $\tilde{\boldsymbol{\beta}}_i = \boldsymbol{\beta}_i - \hat{\boldsymbol{\beta}}_i$, $i = 1, 2$, be the parameter estimation errors.

The projection operator $\dot{\hat{\boldsymbol{\theta}}} = \mathrm{Proj}\{\boldsymbol{\tau}\}$ has the following property

$$-\tilde{\boldsymbol{\theta}}^\top \boldsymbol{\Gamma}^{-\mathbf{1}} \mathrm{Proj}\{\boldsymbol{\tau}\} \leq -\tilde{\boldsymbol{\theta}}^\top \boldsymbol{\Gamma}^{-\mathbf{1}} \boldsymbol{\tau}. \tag{28}$$

By using (19), we have

$$\boldsymbol{B}\boldsymbol{u} = \boldsymbol{B}\hat{\boldsymbol{R}}\bar{\boldsymbol{u}} = \bar{\boldsymbol{u}} + \tilde{\boldsymbol{B}}\hat{\boldsymbol{R}}\bar{\boldsymbol{u}} = \bar{\boldsymbol{u}} + \tilde{\boldsymbol{B}}\boldsymbol{u}, \tag{29}$$

where $\tilde{\boldsymbol{B}} = \boldsymbol{B} - \hat{\boldsymbol{B}}$. The determinant of $\boldsymbol{B}$ matrix will always be positive with the known signs of the parameters and from Assumption 2, where $\det(\boldsymbol{B}) = \beta_{1,1}\beta_{2,2} + \beta_{2,1}\beta_{1,2}$, and from this and also with the projection operator, the matrix $\hat{\boldsymbol{R}}$ does not have any singularities and is defined for all estimated parameters, given that the initial values are chosen positive.

Now the terms $\beta_{1,1}u_1 + \beta_{1,2}u_2$ and $-\beta_{2,1}u_1 + \beta_{2,2}u_2$ in (17) and (18) can be expressed as

$$\boldsymbol{\beta}_1 \boldsymbol{u} = \bar{u}_1 + \tilde{\boldsymbol{\beta}}_1 \boldsymbol{u}, \tag{30}$$

$$\boldsymbol{\beta}_2 \boldsymbol{u} = \bar{u}_2 + \tilde{\boldsymbol{\beta}}_2 \boldsymbol{u}. \tag{31}$$

We define the final Lyapunov function as

$$\begin{aligned} V_2(\boldsymbol{z}, \tilde{\boldsymbol{\beta}}, \tilde{\boldsymbol{\theta}}, t) =& V_1 + \frac{1}{2}z_3^2 + \frac{1}{2}z_4^2 + \frac{1}{2}\tilde{\boldsymbol{\theta}}_1^\top \boldsymbol{\Gamma}_1^{-1}\tilde{\boldsymbol{\theta}}_1 \\ &+ \frac{1}{2}\tilde{\boldsymbol{\theta}}_2^\top \boldsymbol{\Gamma}_2^{-1}\tilde{\boldsymbol{\theta}}_2 + \frac{1}{2}\tilde{\boldsymbol{\beta}}_1 \boldsymbol{\Gamma}_3^{-1}\tilde{\boldsymbol{\beta}}_1^\top + \frac{1}{2}\tilde{\boldsymbol{\beta}}_2 \boldsymbol{\Gamma}_4^{-1}\tilde{\boldsymbol{\beta}}_2^\top . \end{aligned} \tag{32}$$

The derivative of (32) along with (17) to (31) gives

$$\begin{aligned} \dot{V}_2 =& -c_1z_1^2 - c_2z_2^2 - c_3z_3^2 - c_4z_4^2 + \boldsymbol{\phi}_1^\top \tilde{\boldsymbol{\theta}}_1 z_3 \\ &+ \boldsymbol{\phi}_2^\top \tilde{\boldsymbol{\theta}}_2 z_4 - \tilde{\boldsymbol{\theta}}_1^\top \boldsymbol{\Gamma}_1^{-1}\dot{\hat{\boldsymbol{\theta}}}_1 - \tilde{\boldsymbol{\theta}}_2^\top \boldsymbol{\Gamma}_2^{-1}\dot{\hat{\boldsymbol{\theta}}}_2 \\ &+ \tilde{\boldsymbol{\beta}}_1 \boldsymbol{u} z_3 + \tilde{\boldsymbol{\beta}}_2 \boldsymbol{u} z_4 - \tilde{\boldsymbol{\beta}}_1 \boldsymbol{\Gamma}_3^{-1}\dot{\hat{\boldsymbol{\beta}}}_1^\top - \tilde{\boldsymbol{\beta}}_2 \boldsymbol{\Gamma}_4^{-1}\dot{\hat{\boldsymbol{\beta}}}_2^\top \\ =& -c_1z_1^2 - c_2z_2^2 - c_3z_3^2 - c_4z_4^2 \\ &- \tilde{\boldsymbol{\theta}}_1^\top \boldsymbol{\Gamma}_1^{-1}\left(\dot{\hat{\boldsymbol{\theta}}}_1 - \boldsymbol{\Gamma}_1\boldsymbol{\phi}_1 z_3\right) - \tilde{\boldsymbol{\beta}}_1 \boldsymbol{\Gamma}_3^{-1}\left(\dot{\hat{\boldsymbol{\beta}}}_1^\top - \boldsymbol{\Gamma}_3 \boldsymbol{u} z_3\right) \\ &- \tilde{\boldsymbol{\theta}}_2^\top \boldsymbol{\Gamma}_2^{-1}\left(\dot{\hat{\boldsymbol{\theta}}}_2 - \boldsymbol{\Gamma}_2\boldsymbol{\phi}_2 z_4\right) - \tilde{\boldsymbol{\beta}}_2 \boldsymbol{\Gamma}_4^{-1}\left(\dot{\hat{\boldsymbol{\beta}}}_2^\top - \boldsymbol{\Gamma}_4 \boldsymbol{u} z_4\right). \end{aligned} \tag{33}$$

The property of the projection operator in (28) and the update laws (24)-(27) eliminate the last four terms in equation (33). Then

$$\dot{V}_2 \leq -c_1z_1^2 - c_2z_2^2 - c_3z_3^2 - c_4z_4^2. \tag{34}$$

We then have the following stability and performance results based on the control scheme.

Theorem 1: *Considering the closed-loop adaptive system consisting of the plant* (3)*, the adaptive controller* (19)*, the virtual control laws* (13) *and* (14)*, the parameter updating laws* (24)-(27) *and Assumptions 1 and 2. All signals in the closed loop system are ensured to be uniformly bounded. Furthermore, asymptotic tracking is achieved, i.e.*

$$\lim_{t\to\infty} = [x_i(t) - x_{ri}(t)] = 0, \qquad i = 1, 2. \tag{35}$$

Proof: The stability properties of the equilibrium follow from (32) and (34). By applying the LaSalle-Yoshizawa theorem, V_2 is uniformly bounded. This implies that z_1, z_2, z_3, z_4 are bounded and are asymptotically stable and z_1, z_2, z_3, $z_4 \to 0$ as $t \to \infty$ and also $\hat{\boldsymbol{\theta}}_1$, $\hat{\boldsymbol{\theta}}_2$, $\hat{\boldsymbol{\beta}}_1$ and $\hat{\boldsymbol{\beta}}_2$ are bounded. Since $z_1 = x_1 - x_{r1}$ and $z_2 = x_2 - x_{r2}$, tracking of the reference signals is also achieved, and x_1 and x_2 are also bounded since z_1 and z_2 are bounded and since x_{r1} and x_{r2} are bounded by definition, cf. Assumption 1. The virtual controls α_1 and α_2 are also bounded from (13) and (14) and then x_3 and x_4 are also bounded. From (19) it follows that the control inputs also are bounded.

Remark 1: Theorem 1 implies that the error signals will converge to zero. For a real system like the helicopter model, there are disturbances due to e.g. noise from sensors and unmodeled dynamics that are not included in this model, and so the helicopter will have a practical stabilization with the adaptive controller, where the solution is ultimately bounded by a constant μ_0, that is $\|\boldsymbol{z}\| \leq \mu_0, \ \ \forall t \geq T$, for some $T > 0$ [17].

B. Quantized Inputs

Considering the nonlinear state space model with quantized inputs expressed as

$$\dot{\boldsymbol{x}} = \begin{bmatrix} x_3 \\ x_4 \\ \boldsymbol{\phi}_1^\top \boldsymbol{\theta}_1 \\ \boldsymbol{\phi}_2^\top \boldsymbol{\theta}_2 \end{bmatrix} + \begin{bmatrix} 0 \\ 0 \\ \beta_{1,1}q(u_1) + \beta_{1,2}q(u_2) \\ -\beta_{2,1}q(u_1) + \beta_{2,2}q(u_2) \end{bmatrix}, \tag{36}$$

where the control inputs u_1 and u_2 are quantized by the uniform quantizer defined in (8). The change of coordinates and step 1 will be the same as when the inputs are continuous and the virtual control laws are designed as in (13) and (14). In step 2 the control inputs appear, and the derivative of z_3 and z_4 are expressed as

$$\dot{z}_3 = \beta_{1,1}q(u_1) + \beta_{1,2}q(u_2) + \boldsymbol{\phi}_1^\top \boldsymbol{\theta}_1 + c_1(x_3 - \dot{x}_{r1}) - \ddot{x}_{r1}, \tag{37}$$

$$\dot{z}_4 = -\beta_{2,1}q(u_1) + \beta_{2,2}q(u_2) + \boldsymbol{\phi}_2^\top \boldsymbol{\theta}_2 + c_2(x_4 - \dot{x}_{r2}) - \ddot{x}_{r2}. \tag{38}$$

The quantizer inputs are decomposed into two parts

$$q(u_k) = u_k(t) + d_k(t), \tag{39}$$

where d_k is the quantization error and bounded by a constant, $|d_k| \leq \delta_k$, where

$$\delta_k = \max\{u_{k,0} + l_k/2, l_k/2\}. \tag{40}$$

Thus the equations (37) and (38) are expressed as

$$\begin{aligned} \dot{z}_3 =& \beta_{1,1}(u_1 + d_1) + \beta_{1,2}(u_2 + d_2) + \boldsymbol{\phi}_1^\top \boldsymbol{\theta}_1 \\ &+ c_1(x_3 - \dot{x}_{r1}) - \ddot{x}_{r1}, \end{aligned} \tag{41}$$

$$\begin{aligned} \dot{z}_4 =& -\beta_{2,1}(u_1 + d_1) + \beta_{2,2}(u_2 + d_2) + \boldsymbol{\phi}_2^\top \boldsymbol{\theta}_2 \\ &+ c_2(x_4 - \dot{x}_{r2}) - \ddot{x}_{r2}, \end{aligned} \tag{42}$$

where due to quantization, two extra terms are included in each equation. The inputs are designed in the controller (19) together with (21)-(23) and with the parameter updating laws (24)-(27). The final Lyapunov function V_2 is defined as in (32), the same as without quantization. Then the derivative of V_2 gives

$$\begin{aligned} \dot{V}_2 =& -c_1z_1^2 - c_2z_2^2 - c_3z_3^2 - c_4z_4^2 + \boldsymbol{\beta}_1 \boldsymbol{d} z_3 + \boldsymbol{\beta}_2 \boldsymbol{d} z_4 \\ &- \tilde{\boldsymbol{\theta}}_1^\top \boldsymbol{\Gamma}_1^{-1}\left(\dot{\hat{\boldsymbol{\theta}}}_1 - \boldsymbol{\Gamma}_1\boldsymbol{\phi}_1 z_3\right) - \tilde{\boldsymbol{\beta}}_1 \boldsymbol{\Gamma}_3^{-1}\left(\dot{\hat{\boldsymbol{\beta}}}_1^\top - \boldsymbol{\Gamma}_3 \boldsymbol{u} z_3\right) \\ &- \tilde{\boldsymbol{\theta}}_2^\top \boldsymbol{\Gamma}_2^{-1}\left(\dot{\hat{\boldsymbol{\theta}}}_2 - \boldsymbol{\Gamma}_2\boldsymbol{\phi}_2 z_4\right) - \tilde{\boldsymbol{\beta}}_2 \boldsymbol{\Gamma}_4^{-1}\left(\dot{\hat{\boldsymbol{\beta}}}_2^\top - \boldsymbol{\Gamma}_4 \boldsymbol{u} z_4\right), \end{aligned} \tag{43}$$

where $\boldsymbol{d} = [d_1 \ \ d_2]^\top$, and where the property of the projection operator in (28) and the update laws (24)-(27) eliminate the last four terms in equation (43). Then

$$\begin{aligned}\dot{V}_2 \leq & -c_1 z_1^2 - c_2 z_2^2 - c_3 z_3^2 - c_4 z_4^2 + \boldsymbol{\beta}_1 \boldsymbol{d} z_3 + \boldsymbol{\beta}_2 \boldsymbol{d} z_4 \\ \leq & -c_0 \|\boldsymbol{z}\|^2 + \sqrt{(|\boldsymbol{\beta}_1|\boldsymbol{\delta})^2 + (|\boldsymbol{\beta}_2|\boldsymbol{\delta})^2}\|\boldsymbol{z}\| \\ \leq & -(1-\lambda)c_0\|\boldsymbol{z}\|^2 - \lambda c_0 \|\boldsymbol{z}\|^2 + \sqrt{(|\boldsymbol{\beta}_1|\boldsymbol{\delta})^2 + (|\boldsymbol{\beta}_2|\boldsymbol{\delta})^2}\|\boldsymbol{z}\| \\ \leq & -(1-\lambda)c_0\|\boldsymbol{z}\|^2, \quad \forall \|\boldsymbol{z}\| \geq \frac{\sqrt{(|\boldsymbol{\beta}_1|\boldsymbol{\delta})^2 + (|\boldsymbol{\beta}_2|\boldsymbol{\delta})^2}}{\lambda c_0}\end{aligned} \tag{44}$$

where $c_0 = \min\{c_1, c_2, c_3, c_4\}$, the constant $\boldsymbol{\delta} = [\delta_1 \ \ \delta_2]^\top$ is the maximum quantization errors as defined in (40) and $0 < \lambda < 1$. We then have the following stability and performance results based on the control scheme.

Theorem 2: *Considering the closed-loop adaptive system consisting of the plant* (36)*, the adaptive controller* (19)*, the virtual control laws* (13) *and* (14)*, the parameter updating laws* (24)-(27)*, the uniform quantizer* (8) *and Assumptions 1 and 2. All signals in the closed loop system are ensured to be uniformly bounded. The tracking error signals will converge to a compact set, i.e.*

$$\|\boldsymbol{z}\| \leq \mu = \frac{\sqrt{(|\boldsymbol{\beta}_1|\boldsymbol{\delta})^2 + (|\boldsymbol{\beta}_2|\boldsymbol{\delta})^2}}{\lambda c_0}, \tag{45}$$

where μ is a positive constant. The tracking errors $e_i(t) = x_i(t) - x_{ri}(t)$ are ultimately bounded by $\|e_i\| \leq \mu$, and tracking is achieved.

Proof: The stability properties of the equilibrium follows from (32) and (44). The quantization error is bounded by definition (40). By applying the LaSalle-Yoshizawa theorem, V_2 is bounded. This implies that z_1, z_2, z_3, z_4, $\hat{\boldsymbol{\theta}}_1$, $\hat{\boldsymbol{\theta}}_2$, $\hat{\boldsymbol{\beta}}_1$ and $\hat{\boldsymbol{\beta}}_2$ are bounded. Furthermore, z_1, z_2, z_3 and z_4, will converge to a compact set containing the equilibrium as $t \to \infty$. Since $z_1 = x_1 - x_{r1}$ and $z_2 = x_2 - x_{r2}$, the states x_1 and x_2 are also bounded since z_1 and z_2 are bounded and since x_{r1} and x_{r2} are bounded by definition, cf. Assumption 1. Tracking of the reference signals is achieved, with a bounded tracking error. The virtual controls α_1 and α_2 are also bounded from (13) and (14) and then x_3 and x_4 are also bounded. From (19) it follows that the control inputs also are bounded.

Remark 2: The tracking errors are adjustable by tuning the design parameters $c_i, \ i \in \{1, 2, 3, 4\}$.

Remark 3: The smaller quantization intervals l_k, the smaller the compact set for the error variables $\|\boldsymbol{z}\|$ will be, and if l_k decreases to zero and there is no quantization, the error will also be zero and the result will be similar to Theorem 1, without quantization.

Remark 4: The bound for the error system will also include the bound from Remark 1 for the helicopter model, only shifting the bound to $\|\boldsymbol{z}\| \leq \mu_0 + \mu, \quad \forall t \geq T$, for some $T > 0$.

IV. Experimental Results

The Quanser Aero helicopter system shown in Figure 4 is a two-rotor laboratory equipment for flight control-based experiments. The setup is a horizontal position of the main thruster and a vertical position of the tail thruster, which resembles a helicopter with two propellers driven by two DC motors.

The proposed controller was simulated using MAT-LAB/Simulink and tested on the Quanser Aero helicopter system. The initial states were set as $\boldsymbol{x}(0) = 0$ and the design parameters were set as $c_1 = c_2 = 6$, $c_3 = c_4 = 3$, $\boldsymbol{\Gamma}_1 = \boldsymbol{I}_3$, $\boldsymbol{\Gamma}_2 = \boldsymbol{I}_2$ and $\boldsymbol{\Gamma}_3 = \boldsymbol{\Gamma}_4 = 0.01\boldsymbol{I}_2$. The same quantization intervals were used for the two inputs, since the two motors on the helicopter model are equal and where the range of the inputs are similar and in the range of $[-24, 24]$. The interval was chosen $l_1 = l_2 = 1$, and is a quantization level chosen high to show the effect of the quantization, since there are other disturbances that will affect the results as e.g. noise from sensors. The constant $u_{k,0}$ was chosen equal zero for both inputs, and so the upper bound for the quantization errors were $\delta_1 = \delta_2 = l_k/2 = 1/2$. The initial values for the parameters were chosen as $\hat{\boldsymbol{\beta}}_1(0) = [0.0506 \ \ 0.0506]$, $\hat{\boldsymbol{\beta}}_2(0) = [-0.0645 \ \ 0.0810]$, $\hat{\boldsymbol{\theta}}_1(0) = [0.322 \ \ 1.8436 \ \ 0.0007]^\top$ and $\hat{\boldsymbol{\theta}}_2(0) = [0.4374 \ \ 0.0014]^\top$ based on estimates for the values in [18].

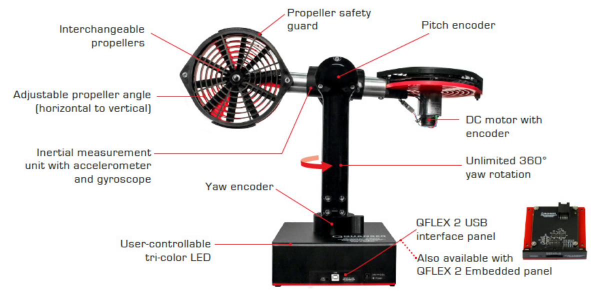

Fig. 4. Quanser Aero, helicopter model

The objective in this test was to track a sinusoidal signal, where a sine wave with amplitude of 40 degrees and frequency of 0.05 Hz was applied to pitch, while there should be no rotation about yaw, and see how the system was affected by quantization of inputs.

A. Results without Quantization

The results from simulation and testing on the helicopter with continuous inputs are shown in Figures 5-6, where red plots are from simulation and blue plots are from the real system. While the simulations in Figure 5 show that the tracking errors converge to zero, we see that for the helicopter, the tracking errors converge to bounded errors close to zero. This is due to the unknown disturbances affecting the system as in Remark 1. Tracking of the reference signal is achieved, for both pitch and yaw angle. The inputs are also plotted in Figure 5.

In Figure 6, the norm of $\boldsymbol{z}$ is plotted. The simulation shows that $\|\boldsymbol{z}\| \to 0$ as $t \to \infty$, while this is not the case for the

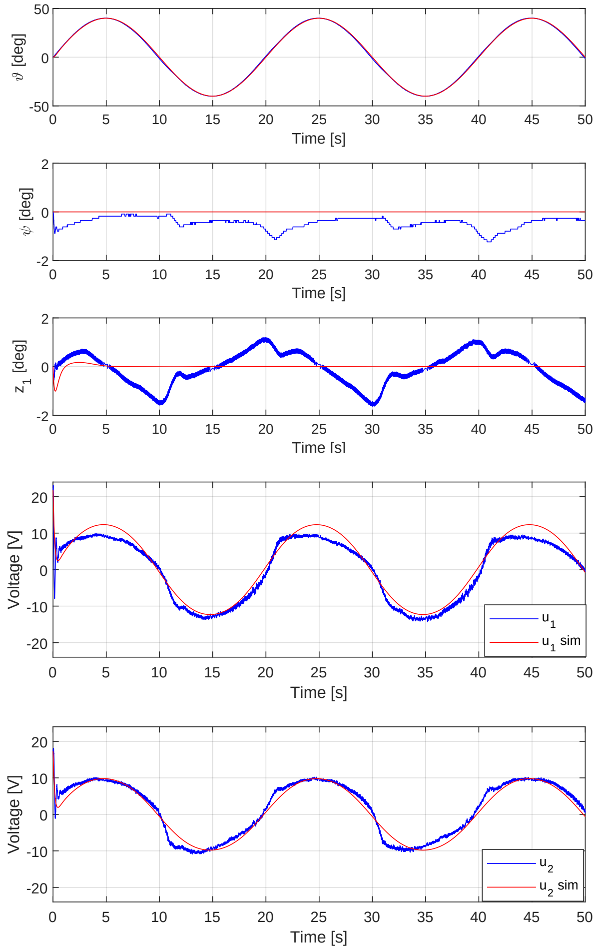

Fig. 5. Results without quantization. 1) Pitch angle. 2) Yaw angle. 3) Pitch angle error. 4) Inputs.

real system. From the plot for the helicopter system, we define $\mu_0 = \max\|\boldsymbol{z}\|$.

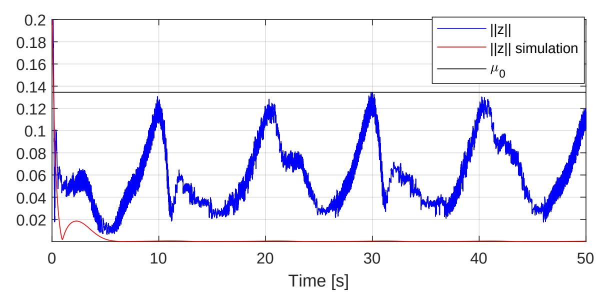

Fig. 6. Norm of z without quantization.

B. Results with Quantization

Now the inputs were quantized, with results plotted in Figures 7-9. From Figure 7, we can see that the desired trajectory for a sine wave in pitch can be followed using the proposed adaptive controller both in simulation and testing on the helicopter system. From the simulation, there is an error

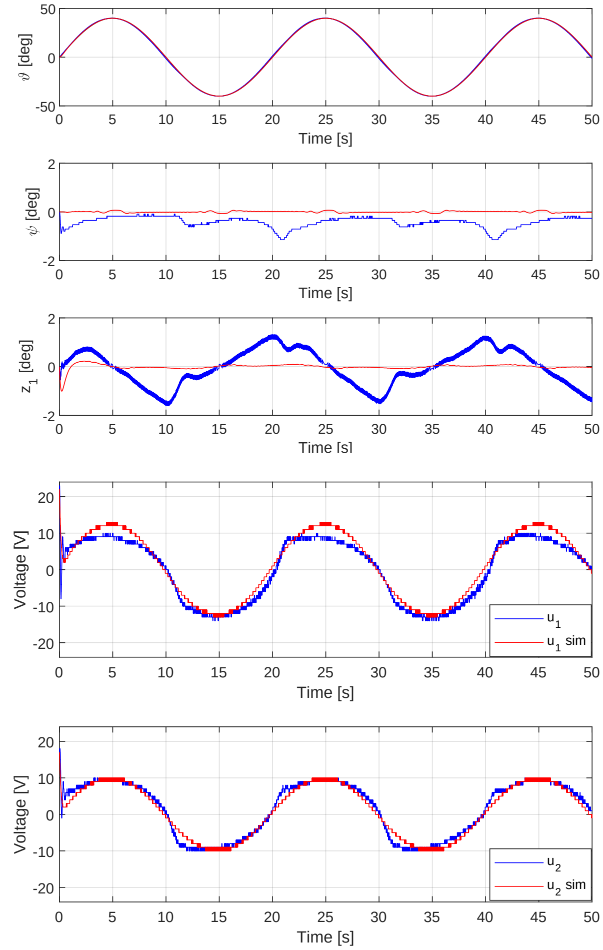

Fig. 7. Results with quantization. 1) Pitch angle. 2) Yaw angle. 3) Pitch angle error. 4) Inputs.

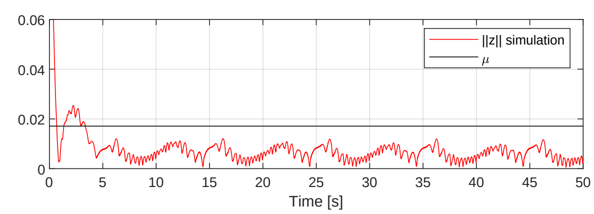

Fig. 8. Simulation of norm of z with quantization and the bound μ.

for both angles due to quantization compared to simulation without quantization in Figure 5. In Figure 8, the norm of the error state $\boldsymbol{z}$ is plotted and also the bound μ from Theorem 2, computed with $\lambda = 0.999$, and assuming $\boldsymbol{\beta}_1 = \hat{\boldsymbol{\beta}}_1(0)$ and $\boldsymbol{\beta}_2 = \hat{\boldsymbol{\beta}}_2(0)$. In the transient period, the norm enters the bound, but leaves it for a short period, and this is possible due to the LaSalle-Yoshizawa theorem. After this it remains within the bound μ. Looking at the plotted norm for the helicopter in Figure 9, where μ_0 is the bound found without quantization due to unknown disturbances and $\mu_0 + \mu$ also includes the bound for quantization, we see that $\|\boldsymbol{z}\|$ is within the bound for the whole time period.

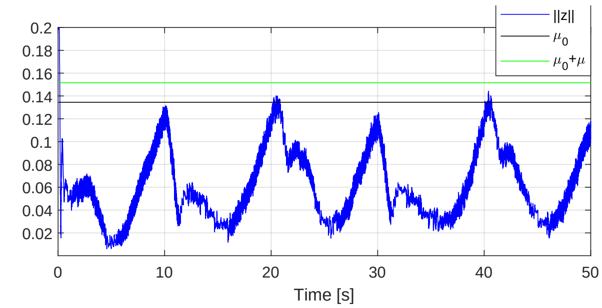

Fig. 9. Norm of z with quantization from the helicopter, with bounds.

C. Comparing Results

To compare the results with and without quantization, the total tracking error, z_{track}, and the total voltage used, u_{total}, was measured, where

$$z_{track} = \sum_{i=1}^{2} \int_0^t z_i(\tau)^2 d\tau, \tag{46}$$

$$u_{total} = \sum_{i=1}^{2} \int_0^t u_i(\tau)^2 d\tau, \tag{47}$$

with $t = 50\ s$. There is a trade-off between the error and voltage consumption since the more accurate the controller is, the more voltage is needed to hold the trajectory closer to the reference.

In Table I, the results are compared for different quantization intervals. The tracking error is higher when the inputs are quantized, while the total voltage use is lower for most of the tests with quantization. The higher error is due to the quantization error, as expected from Theorems 1 and 2.

TABLE I
COMPARISON OF ERROR AND VOLTAGE USE WITH AND WITHOUT QUANTIZATION

Measurement	**Quantization**				
	$l_k = 0$	$l_k = 0.1$	$l_k = 0.5$	$l_k = 1$	$l_k = 1.5$
z_{track}	0.0110	0.0116	0.0114	0.0116	0.0121
u_{total}	6429	6444	6365	6367	6328

V. CONCLUSION

In this paper, an adaptive backstepping control scheme is considered for a MIMO nonlinear helicopter model with input quantization. The system parameters are not required to be fully known for the controller design. A theoretical proof of stability is given with the use of constructed Lyapunov functions, where boundedness of all signals in the closed loop system are achieved and also tracking of a given reference signal. The tracking error signals will converge to a compact set. Experiments and simulations validates the proof, where tracking is achieved and the total tracking error signals are some higher when the inputs are quantized compared to when inputs are not quantized.

REFERENCES

[1] X. Ge, F. Yang, and Q.-L. Han, "Distributed networked control systems: A brief overview," *Information Sciences*, vol. 380, pp. 117–131, Feb. 2017.
[2] X.-M. Zhang, Q.-L. Han, X. Ge, D. Ding, L. Ding, D. Yue, and C. Peng, "Networked control systems: A survey of trends and techniques," *IEEE/CAA Journal of Automatica Sinica*, vol. 7, no. 1, 2020.
[3] D. Zhang, P. Shi, Q.-G. Wang, and L. Yu, "Analysis and synthesis of networked control systems: A survey of recent advances and challenges," *ISA Transactions 66*, pp. 376–392, 2017.
[4] Z. P. Jiang and T. F. Liu, "Quantized nonlinear control - a survey," *Acta Automatica Sinica*, vol. 39, no. 11, pp. 1820–1830, Nov. 2013.
[5] N. Elia and S. K. Mitter, "Stabilization of linear systems with limited information," *IEEE Transactions on Automatic Control*, vol. 46, no. 9, pp. 1384–1400, Sep. 2001.
[6] S. Tatikonda and S. Mitter, "Control under communication constraints," *IEEE Transactions on Automatic Control*, vol. 49, no. 7, pp. 1056–1068, Jul. 2004.
[7] M. Fu and L. Xie, "The sector bound approach to quantized feedback control," *IEEE Transactions on Automatic Control*, vol. 50, no. 11, pp. 1698–1711, Nov. 2005.
[8] C. D. Persis, "Robust stabilization of nonlinear systems by quantized and ternary control," *Systems & Control Letters*, vol. 58, pp. 602–608, 2009.
[9] J. Zhou, C. Wen, and W. Wang, "Adaptive control of uncertain nonlinear systems with quantized input signal," *Automatica*, vol. 95, pp. 152–162, 2018.
[10] J. Zhou and W. Wang, "Adaptive control of quantized uncertain nonlinear systems," *IFAC PapersOnLine*, vol. 50, no. 1, pp. 10 425–10 430, 2017.
[11] J. Zhou, C. Wen, W. Wang, and F. Yang, "Adaptive backstepping control of nonlinear uncertain systems with quantized states," *IEEE Transactions on Automatic Control*, vol. 64, no. 11, pp. 4756–4763, Nov. 2019.
[12] J. Zhou and C. Wen, "Adaptive backstepping control of uncertain nonlinear systems with input quantization," in *IEEE Conference on Decision and Control*, Dec. 2013, pp. 5571–5576.
[13] J. Zhou, "Decentralized adaptive control for interconnected nonlinear systems with input quantization," *IFAC PapersOnLine*, vol. 50, no. 1, pp. 10 419–10 424, 2017.
[14] H. Sun, N. Hovakimyan, and T. Basar, "$\mathcal{L}_1$ adaptive controller for uncertain nonlinear multi-input multi-output systems with input quantization," *IEEE Transactions on Automatic Control*, vol. 57, no. 3, pp. 565–578, 2012.
[15] M. Krstić, I. Kanellakopoulos, and P. Kokotović, *Nonlinear and Adaptive Control Design*. John Wiley & Sons, Inc., 1995.
[16] S. M. Schlanbusch and J. Zhou, "Adaptive backstepping control of a 2-dof helicopter," in *Proceedings of the IEEE 7th International Conference on Control, Mechatronics and Automation*, 2019.
[17] H. K. Khalil, *Nonlinear Control*. Pearson, 2015.
[18] S. M. Schlanbusch, "Adaptive backstepping control of quanser 2dof helicopter - theory and experiments," Master's thesis, University of Agder, 2019.